Polymer 245 (2022) 124671

Contents lists available at ScienceDirect

Polymer

journal homepage: www.elsevier.com/locate/polymer

Dielectric relaxation and glassy dynamics in poly(diisopropyl fumarate) and its copolymers with acrylate segments

Kairi Miyata [a], Jun Yoshioka [a], Koji Fukao [a,*], Yasuhito Suzuki [b], Akikazu Matsumoto [b]

[a] Department of Physics, Ritsumeikan University, Noji-Higashi 1-1-1, Kusatsu, Shiga, 525-8577, Japan
[b] Department of Applied Chemistry, Graduate School of Engineering, Osaka Prefecture University, 1-1 Gakuen-cho, Naka-ku, Sakai, Osaka, 599-8531, Japan

ARTICLE INFO

Keywords:
Dielectric relaxation
X-ray scattering
Poly(diisopropyl fumarate)
Copolymers with acrylate segments

ABSTRACT

Dynamical behavior and glass transitions in copolymers of diisopropyl fumarate (DiPF) with 1-adamantyl acrylate (AdA) or n-butyl acrylate (nBA) are investigated by dielectric relaxation spectroscopy (DRS) to elucidate the effect of structural constraint due to the absence of a CH_2 spacer on the dynamics. DRS measurements revealed that the two copolymers exhibit three dynamical processes: α-, β-, and γ-processes. The relaxation time of the β-process can be described by the Vogel-Fulcher-Tammann (VFT) law in addition to the α-process. Hence, two glass transition temperatures, T_g, can be evaluated from α- and β-processes. The AdA and nBA fraction dependence of T_gs is consistent with that obtained by dynamical mechanical analysis. The Vogel temperature of the α-process is nearly equal to that of the β-process for the PDiPF homopolymer. With the increase in the AdA fraction, the difference in the Vogel temperature between the α- and β-processes increases. This result suggested that there is an intrinsic correlation between the α- and β-processes for PDiPF, and the correlation changes with the AdA fraction. From the nBA fraction dependence of the β-process, the β-process of PDiPF can be related to the segmental motion of the main chain. Nevertheless, PDiPF exhibits a solid-like property up to the T_g, which is related to the α-process. The physical origins of other processes also were discussed.

1. Introduction

Polymeric materials exhibit characteristic dynamical properties depending on the spatial and temporal scales, that is, hierarchical structure of the dynamics [1,2]. There are several dynamical processes that are related to specific structural details, e.g., α-, β-, and γ-processes. Glass transition is one of the most important dynamical phenomena in amorphous materials, where the isotropic liquid state changes into the glassy state without crystalline order [3,4]. The slowing down of the α-process is regarded as the physical origin of the glass transition, and the characteristic time of the α-process increases anomalously on approaching the glass transition temperature, T_g, which is described by the Vogel-Fulcher-Tammann (VFT) law [5–8]. In polymeric systems, segmental motion is the microscopic origin of the α-process. In addition to the α-process, the β-process is typically observed in amorphous materials, which is located at regions where the frequency is higher than that at regions for the α-process at a given temperature. Depending on polymeric systems, side-chain motion [1], local-mode relaxation [9,10], and Johari-Goldstein process [11–14] are possible candidates for the origin of the β-process.

Locations of dynamical processes for polymeric material are plotted in a dispersion map, that is, a plot of frequency vs. the inverse of temperature. If two dynamical processes are located on different places in the dispersion map, they might be regarded as independent dynamical processes in some cases. Nevertheless, several studies on possible correlations between different processes, for example, the α- and β-processes of poly(alkyl methacrylate) have been reported [15,16]. The mechanism elucidation of such correlations between the α- and β-processes is expected to be crucial to understand the nature of the glass transition in amorphous materials.

Dynamical properties of polymeric systems are expected to be controlled by the structure or architecture of polymer chains and by the imposed geometrical constraint [17,18]. Owing to their industrial importance, the dynamics of polyacrylates, belonging to poly(monosubstituted ethylene) with a general formula of $(\text{-}CH_2CHR\text{-})_n$, have been investigated widely by many experimental techniques [19–23]. On the other hand, dynamical properties of poly(1,2-disubstituted ethylene) with a general formula of $(\text{-}CHR\text{-}CHR\text{-})_n$, including poly(dialkyl fumarate), have not been investigated completely yet, because this polymer has been synthesized efficiently only by the radical polymerization of

* Corresponding author.
E-mail address: kfukao@se.ritsumei.ac.jp (K. Fukao).

https://doi.org/10.1016/j.polymer.2022.124671
Received 10 November 2021; Received in revised form 16 February 2022; Accepted 18 February 2022
Available online 25 February 2022

some dialkyl fumarate [24–27]. The key structural property of this polymer is the absence of methylene spacer (-CH_2-) in the backbone chain (See Fig. 1). Owing to this structural constraint, poly(1,2-disubstituted ethylene) is expected to form a rigid chain structure with large potential energy barrier against the rotation around the backbone chain [28,29] and to induce a dynamical anomaly compared with the dynamics of vinyl polymers.

In our previous studies, dynamics and structure of poly(diisopropyl fumarate) (PDiPF), which is a typical example of poly(1,2-disubstituted ethylene), and its copolymers with acrylate segments have been investigated by various experimental techniques [30,31]. For PDiPF, various dynamical processes, i.e., the α-, β-, and γ-processes, have been reported to be observed by dynamical mechanical measurements [32]. Our preliminary dielectric relaxation spectroscopy (DRS) measurement revealed that the temperature dependence of the relaxation time of the β-process can be described by the VFT law in the same way as that observed for the α-process [31]. This "unusual" property of the β-process might originate from the steric constraint induced by the absence of a methylene spacer. Moreover, a strong correlation between the α- and β-processes is expected, because both processes are described by the VFT law. Details of the correlation should be clarified to investigate the origin of the hierarchical structure of the dynamics of polymeric systems. Furthermore, the relation between the γ-process and other processes still needs to be clarified.

It should be noted here that in the literatures on PDiPF, the three dynamical processes are called α-, β-, and γ-processes in order from high temperature to low temperature. Hence, the same notation is used also in this paper to avoid possible confusion. The physical origin of the processes will be discussed later.

In this study, a series of random copolymers of diisopropyl fumarate (DiPF) and 1-adamantyl acrylate (AdA) or n-butyl acrylate (nBA) with various fractions are prepared. Here, PDiPF is classified as poly(1,2-disubstituted ethylene), and PAdA and PnBA are classified as poly (monosubstituted ethylene). Dynamical properties are investigated by DRS, in addition to structural investigation by X-ray scattering, to elucidate changes in the dynamics and structure of PDiPF with the increase in the fraction of acrylate segments. This study is expected to clarify how a steric constraint induced by the absence of a methylene spacer affects the dynamical behavior of polymers.

Sec. 2 provides experimental details, such as sample preparation, X-ray scattering and DRS measurements. Sec. 3 shows the experimental results obtained from X-ray scattering and DRS, as well as discussions on dynamical properties of the three processes using the VFT law, glass transition temperature, Vogel temperature, and the fragility index. Finally, possible origins for these processes are discussed.

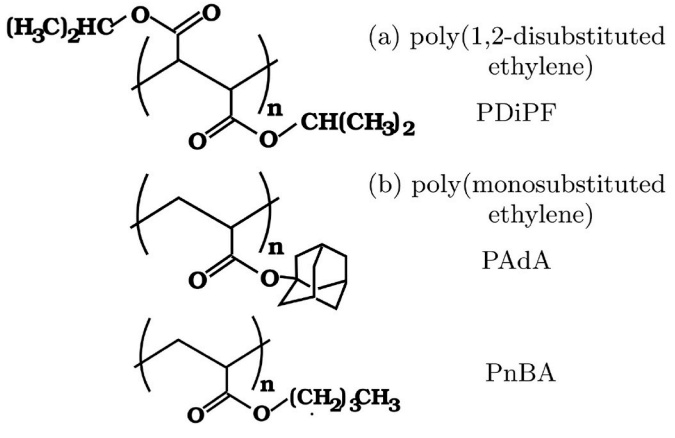

Fig. 1. Chemical structure of (a) poly(diisopropyl fumarate) (PDiPF) as an example of poly(1,2-disubstituted ethylene) and (b) poly(1-adamantyl acrylate) (PAdA) and poly(n-butyl acrylate) (PnBA), which are acrylate polymers, as examples of poly(monosubstituted ethylene).

2. Experimentals

2.1. Sample preparations

DiPF (Fujifilm Wako Pure Chemical Corporation, Tokyo, Japan) and nBA (Tokyo Chemical Industry Corporation, Ltd, Tokyo, Japan) were distilled under reduced pressure prior to use. AdA was provided from Osaka Organic Chemical Industry Ltd, Osaka, Japan and was purified by recrystallization in n-hexane before use. The procedures of the synthesis of random copolymers of DiPF and AdA and characteristics of the synthesized polymers are provided in Ref. [30]. Table 1 summarizes the molecular weights and molecular-weight distributions of the copolymers used herein. Fig. 1 shows the chemical structures of PDiPF, PAdA, and PnBA. The copolymers used in this study are random copolymers.

2.2. X-ray scattering measurements

X-ray scattering measurements were performed at BL40B2 of SPring-8 to investigate the structural order in copolymers P(DiPF/AdA) and P(DiPF/nBA). Simultaneous measurements of small-angle X-ray scattering (SAXS) and wide-angle X-ray scattering (WAXS) were performed, with the camera lengths of 2301 mm and 98.0 mm, respectively, and the X-ray wavelength was 0.09 nm. A Pilatus3S 2 M detector system was used for SAXS, while a flat panel was used for WAXS. Two-dimensional intensity data were converted into one-dimensional intensity as a function of the modulus of the scattering vector q after circular averaging.

2.3. Dielectric relaxation spectroscopy

For DRS measurements, thin films of copolymers P(DiPF/AdA) and P(DiPF/nBA) were prepared by solution casting from a toluene solution of the copolmyers on a brass disk electrode with a diameter of 30 mm. The upper electrode with a diameter of 20 mm was placed on casted polymer films. Between the two electrodes, a 12.5-μm thick Kapton film with a

Table 1
Fraction, molecular weight M_w, dispersity M_w/M_n, T_{DSC}, and activation energy of the γ-process U of homopolymer PDiPF and PAdA, and copolymers P(DiPF/AdA) and P(DiPF/nBA) used in this study. The values of T_{DSC} for P(DiPF/AdA) were measured during heating process (left) and cooling process (right) at the rate of 10 K/min by DSC, while those for P(DiPF/nBA) were measured during heating process at the same rate [30].

Acrylate	DiPF/Acrylate (mol/mol)	$M_w/10^4$	M_w/M_n	T_{DSC} (K)	U(kJ/mol) γ-process	Abrev.
AdA	100/0	12	1.5	343, 338	1.55 ± 0.03	PDiPF
	65/35	32	2.3	381, 372	1.41 ± 0.03	AdA35
	46/54	30	3.1	393, 384	1.27 ± 0.03	AdA54
	35/65	24	4.8	395, 383	1.10 ± 0.03	AdA65
	0/100	25	1.5	423, 410	0.93 ± 0.01	PAdA
nBA	100/0	12	1.5	343	1.55 ± 0.03	PDiPF
	89/11	11	1.7	339	1.68 ± 0.05	nBA11
	78/22	7.6	1.8	331	1.75 ± 0.05	nBA22
	64/36	7.6	2.1	273	2.18 ± 0.11	nBA36
	35/65	11	2.7	256	1.72 ± 0.01	nBA65
	19/81	18	4.5	220	–	nBA81

small area was inserted as a spacer. An impedance analyzer, Alpha-A high-performance frequency analyzer, was used together with a cooling unit, a Quatro cryosystem, from Novocontrol Technologies GmbH & Co. KG (Montabaur, Germany) [33]. A liquid parallel-plate sample cell (Novocontrol, BDS1308) was used only for measurements of P(DiPF/nBA) with an nBA fraction of greater than 65%, because copolymers with this fraction of nBA are liquid at room temperature. Dielectric measurements were performed in the frequency range f from 40 mHz to 1 MHz and at a temperature range T from 493 K to 173 K. After correcting for the thickness and area of the electrode, complex dielectric permittivity ϵ^* was obtained as a function of the angular frequency $\omega(\equiv 2\pi f)$ and the temperature T. Here, complex dielectric permittivity is expressed as follows:

$$\epsilon^*(\omega) = \epsilon'(\omega) - i\epsilon''(\omega), \tag{1}$$

where ϵ' and ϵ'' are the real and imaginary parts of complex dielectric permittivity, respectively.

3. Results and discussions

3.1. X-ray scattering

Simultaneous WAXS and SAXS measurements were performed for P(DiPF/AdA) and P(DiPF/AdA) with various fractions of AdA or nBA. As for SAXS measurements, significant scattering signals related to the structure are not observed in the q range from 0.05 nm^{-1}–2.5 nm^{-1}. Fig. 2 shows the X-ray scattering intensity as a function of the modulus of the scattering vector q in the WAXS region for P(DiPF/AdA) and P(DiPF/nBA). Only broad peaks are observed in WAXS region. Hence, there is no crystalline order in copolymer systems based on the results obtained from WAXS and SAXS measurements.

For PDiPF, two peaks are observed at 5.94 nm^{-1} and 13.4 nm^{-1}, which correspond to 1.06 nm and 0.47 nm in the real space, respectively (Please check purple curves). A length of 1.06 nm is comparable to the average cross-sectional diameter of the PDiPF chain [31]. The peak at 13.4 nm^{-1} corresponds to the second-ordered peak of the peak at 5.94 nm^{-1} with broader peak width. Owing to the high rotational hindrance around the main chain, the PDiPF chain could be rigid; as a result, PDiPF chains exhibit better packing with a short-range order, and its longer coherence length is greater than that of acrylate polymers.

For PAdA (AdA = 100%), one broad peak is observed at 11.2 nm^{-1}, corresponding to 0.56 nm (See red curve in Fig. 2(a)). In addition, this length is comparable to the averaged diameter of the PAdA chain. The width of the peak at 11.2 nm^{-1} of PAdA is broader than that of the first peak of PDiPF, suggesting that the chain packing in PDiPF is better than that in PAdA. With the increase in the AdA fraction, the scattering profile of P(DiPF/AdA) copolymers continuously changes from that of PDiPF to that of PAdA. With the increase in the AdA fraction, the peak intensity at 5.9 nm^{-1} decreases, while that at 12–13 nm^{-1} increases. At the same time, the position of the second peak shifts continuously from 13.4 nm^{-1}–11.2 nm^{-1}. This result clearly suggested that the chain packing changes continuously with the increase in the AdA fraction.

For P(DiPF/nBA) copolymers with an nBA fraction up to 81%, two peaks are observed at 5.9 nm^{-1} and 13 nm^{-1}, respectively. PnBA homopolymers exhibit two peaks in the WAXS pattern, where the intensity of the first peak is considerably less than that of the second peak [34]. The second peak position corresponds to the averaged diameter of the PnBA chain. The packing of the PnBA chains fits extremely well with that of the PDiPF chains such that the positions of the two peaks in the WAXS pattern do not change even with the change in the nBA fraction, although the intensity ratio of the two peaks changes. Hence, the local packing structure in P(DiPF/nBA) does not change considerably with the nBA fraction.

3.2. Dielectric relaxation spectroscopy

Dielectric relaxation spectroscopy measurements were performed for P(DiPF/AdA) and P(DiPF/nBA) copolymers with various fractions of AdA or nBA to obtain the frequency and temperature dependence of complex dielectric permittivity. First, Figs. 3 and 4 show the results obtained for P(DiPF/AdA). Figs. S1 and S2 in the Supplemental Material show similar results for P(DiPF/nBA).

Fig. 3 shows the frequency dependence of the imaginary part of complex dielectric permittivity ϵ'' at various temperatures for P(DiPF/AdA) copolymers with three AdA fractions of 0%, 54%, and 100%, respectively. Fig. 3 shows the three processes: α-, β-, and γ-processes. Here, we assume that each dynamical process can be described by the Havriliak-Negami (HN) empirical equation [35], and also, there is contribution from DC conductivity [36]. Complex dielectric permittivity can be expressed by the following equation:

$$\epsilon^*(\omega) = \epsilon_\infty + i\frac{\sigma_0}{\epsilon_0\omega} + \sum_{i=\alpha,\beta,\gamma}\frac{\Delta\epsilon_i}{(1+(i\omega\tau_i)^{\alpha_i})^{\beta_i}}, \tag{2}$$

where ϵ_∞ is the dielectric permittivity at an extremely high frequency, ϵ_0 is the dielectric permittivity in vacuo, and σ_0 is the DC conductivity. $\Delta\epsilon_i$, τ_i, α_i, and β_i correspond to the dielectric strength, relaxation time, shape parameter for peak width, and shape parameter for peak asymmetry of the i-process, respectively. Here, $i = \alpha$, β, and γ.

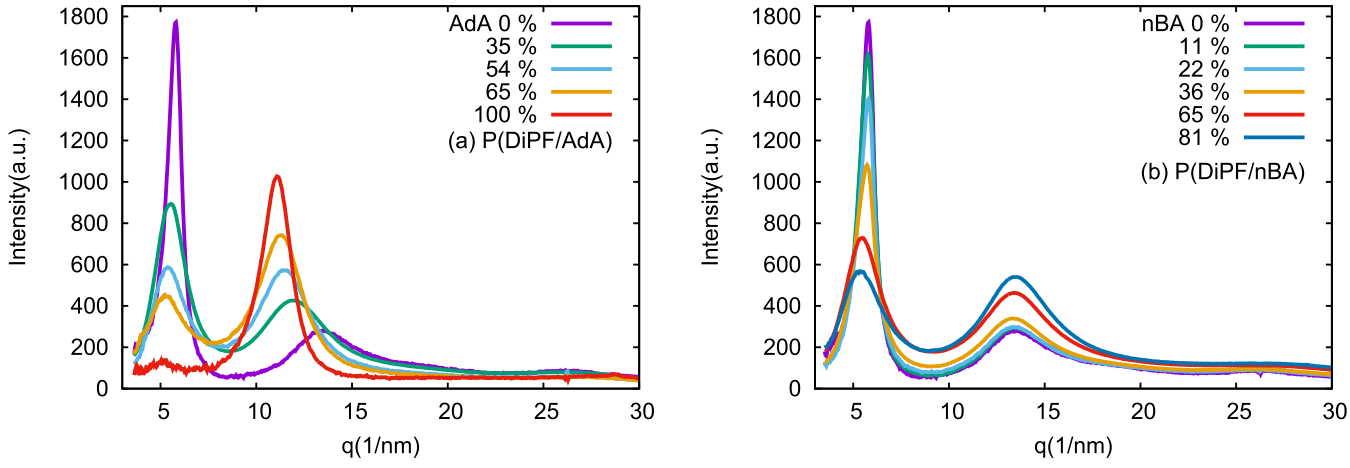

Fig. 2. The dependence of the X-ray scattering intensity in the WAXS region for (a) DiPF/AdA copolymers with various fractions of AdA and (b) DiPF/nBA copolymers with various fractions of nBA. The curves are obtained after circular averaging the 2-D intensity data.

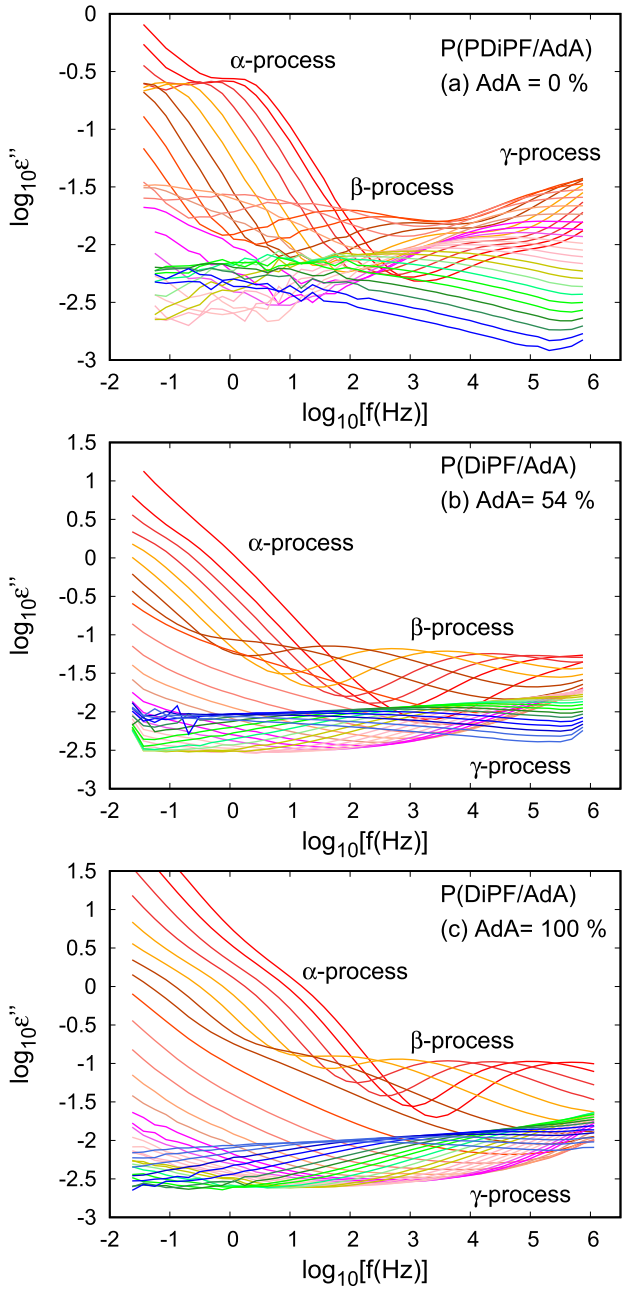

Fig. 3. Dielectric loss spectra at a fixed temperature for DiPF/AdA copolymers with different fractions of AdA contents of 0%, 54%, and 100%, respectively. α-, β-, and γ-processes could be observed depending on the temperature. From the right curve to the left curve, the temperature changes by a step of 10 K (a) from 473 K (red) to 173 K (blue), (b) from 483 K (red) to 153 K (blue), and (c) from 483 K (red) to 153 K (blue). (For interpretation of the references to color in this figure legend, the reader is referred to the Web version of this article.)

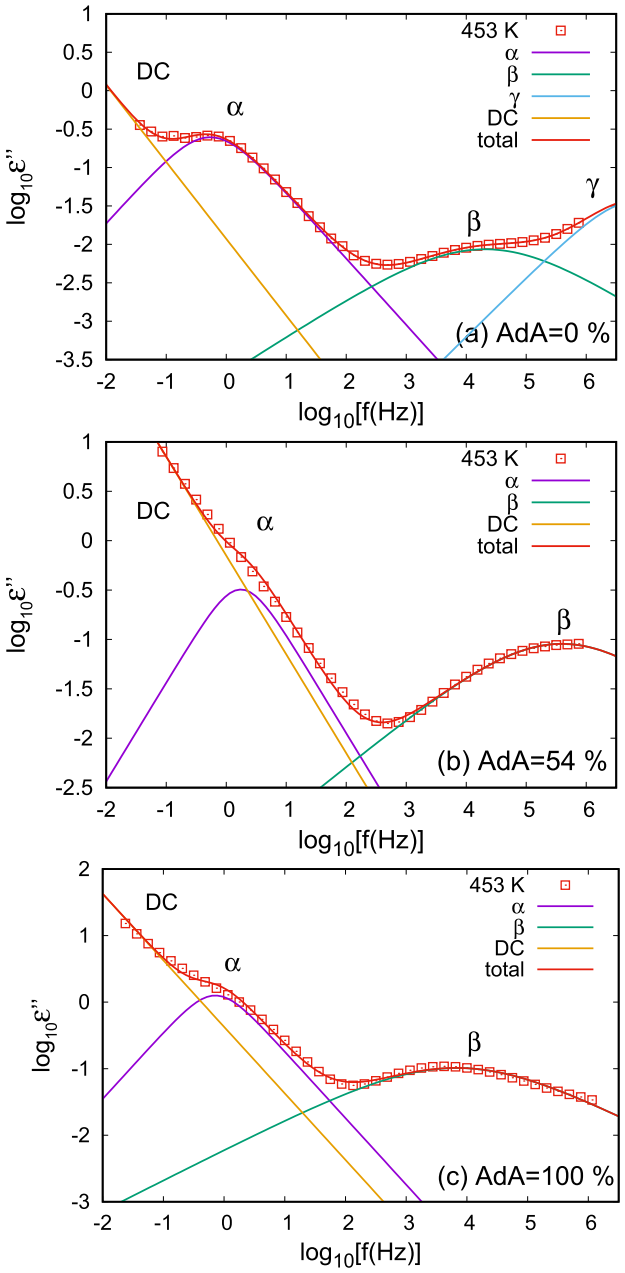

Fig. 4. Dielectric loss spectra at 453 K for DiPF/AdA copolymers including various contributions from the α- (purple), β- (green), and γ-processes(light blue), in addition to DC conductivity. Fitting curves are evaluated by Eq. (2). AdA fractions are (a) 0%, (b) 54%, and (c) 100%. (For interpretation of the references to color in this figure legend, the reader is referred to the Web version of this article.)

Using Eq. (2), the observed frequency dependence of ϵ'' at a given temperature can well be fitted (Fig. 4). The calculated curves for different processes are described with different colors, and the calculated curve for overall values of ϵ'' is indicated by the red curve. From the fitting parameters τ_i, α_i, and β_i, the peak frequency for the i-process $f_{\max,i}$ can be evaluated as follows [36,38]:

$$f_{\max,i} = \frac{1}{2\pi\tau_i}\left(\frac{\sin\frac{\pi}{2}\frac{\alpha_i}{\beta_i+1}}{\sin\frac{\pi}{2}\frac{\alpha_i\beta_i}{\beta_i+1}}\right)^{\frac{1}{\alpha_i}}. \quad (3)$$

Here, $f_{\max}$ can be regarded as the relaxation rate of dynamical processes. If $\beta_i = 1$, the relaxation time of the i-process τ_i and relaxation $f_{\max}$ satisfy the following relation:

$$\tau_i = \frac{1}{2\pi f_{\max,i}}, \quad (4)$$

where $i = \alpha$, β, and γ, and τ_i is the parameter evaluated using the HN equation.

By collating the fitting parameters for various fractions of acrylate segments, the dispersion map for polymer dynamics can be produced as shown in Fig. 5. Here, the logarithm of the relaxation rate f_{max} of the α-, β-, and γ-processes is expressed as a function of the inverse of the absolute temperature $1/T$ for copolymers (a) P(DiPF/AdA) with an AdA fraction in the range from 0% to 100%, and (b) P(DiPF/nBA) with an nBA fraction in the range from 0% to 81%. In this dispersion map, three dynamical processes are separately located, and their locations considerably change with the acrylate fractions. Notably, data for PnBA (nBA fraction = 100%) are added in Fig. 5(b) from Ref. [37]. Dynamical properties of the three processes are discussed in the following sections using the relaxation rate in Fig. 5.

3.3. α- and β-processes

Here, dynamical properties of the α- and β-processes will be discussed. Fig. 6 shows the relaxation rate of the α- and β-processes as a function of $1/T$ for P(DiPF/AdA) with five AdA fractions, which are extracted from Fig. 5(a). The curves in Fig. 6 are obtained from the data fitting using the VFT equation [5–8]:

$$f_{\max,\ i}(T) = f_{0,i}\exp\left(-\frac{U_i}{T - T_{0,i}}\right), \tag{5}$$

where $i = \alpha$ or β and $f_{0,i}$, U_i are positive constants, and $T_{0,i}$ is the Vogel temperature at which the relaxation time of the i-process diverges.

As shown by fitting curves using Eq. (5), *the temperature dependence of the relaxation times of not only the α-process but also the β-process can well be reproduced by the VFT law*, suggesting that the relaxation times of both processes can be diverged at finite temperatures, that is, the Vogel temperature $T_{0,\alpha}$ or $T_{0,\beta}$, during the cooling process.

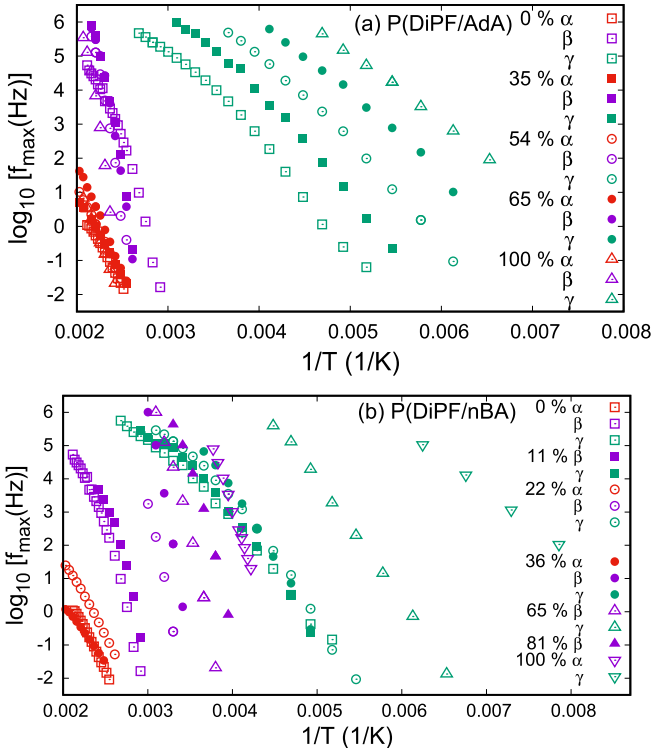

Fig. 5. Dispersion map of three relaxation processes observed for (a) P(DiPF/AdA) with various fractions of AdA and (b) P(DiPF/nBA) with various fractions of nBA using dielectric relaxation spectroscopy. The red, purple, and green symbols show the relaxation rate f_{max} of the α-, β-, and γ-processes as a function of the inverse of absolute temperature, respectively. The data for PnBA in Ref. [37] are added in this dispersion map (b) as a reference of nBA = 100% (See open down triangles). (For interpretation of the references to color in this figure legend, the reader is referred to the Web version of this article.)

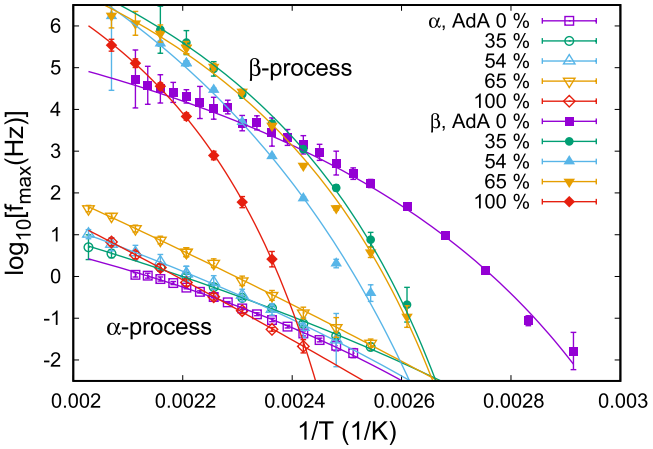

Fig. 6. Relaxation rate of the α- and β-processes as a function of the inverse of temperature for DiPF/AdA copolymers with various AdA fractions. The curves are obtained using Eq. (5).

Furthermore, two glass transition temperatures $T_{g,\alpha}$ and $T_{g,\beta}$ can be well defined from the temperature dependence of the relaxation times of the α- and β-processes as follows. From the data fitting of the relaxation rate of the α- and β-processes via Eq. (5), the three parameters, $f_{0,i}$, U_i, and $T_{0,i}$ can be obtained for each process. Using these parameters, the glass transition temperature $T_{g,\alpha}(T_{g,\beta})$ can be evaluated as the temperature at which the relaxation time of the α-process, τ_α (β-process, τ_β) reaches a macroscopic time scale, τ_g, for example, $\tau_g = 10^2$ s: $\tau_\alpha(T_{g,\alpha}) = \tau_\beta(T_{g,\beta}) = 10^2$ s.

For P(DiPF/nBA), the same data fitting was performed for the α- and β-processes, and the relaxation rates of both processes can be reproduced well by the VFT law in a manner similar to that observed for P(DiPF/AdA). Please check Fig. S3 in the Supplemental Material.

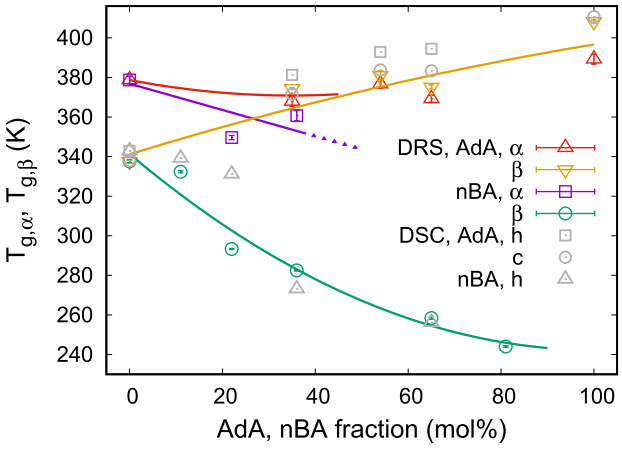

Fig. 7. AdA or nBA fraction dependence of the glass transition temperature $T_{g,\alpha}$ and $T_{g,\beta}$ evaluated from the temperature dependence of the relaxation rate of the α- and β-processes for P(DiPF/AdA) and P(DiPF/nBA). Here, T_g is defined as the temperature at which the relaxation time $\tau_\alpha(\tau_\beta)$ is equal to 10^2 s. The temperatures T_{DSC} at which thermal anomaly is observed by DSC measurements are also plotted; □ and ○ stand for the T_{DSC} measured for the heating and cooling processes for P(DiPF/AdA), respectively, and △ stands for the T_{DSC} for the heating process for P(DiPF/nBA).

3.3.1. Glass transition temperature and Vogel temperature

Fig. 7 shows the AdA or nBA fraction dependence of the glass transition temperatures evaluated from the relaxation times of the α- and β-processes. The $T_{g,\alpha}$ and $T_{g,\beta}$ are 379 K and 338 K for PDiPF, respectively (Fig. 7). With the increase in the AdA fraction up to 36%, the $T_{g,\alpha}$ first decreases and then increases for P(DiPF/AdA) copolymers (See the red triangle △). However, with the increase in the AdA fraction, the $T_{g,\beta}$ increases monotonically (please check the orange down triangle ▽). Furthermore, for PDiPF, $T_{g,\alpha}$ and $T_{g,\beta}$ can be observed separately, while for the AdA fraction greater than 36%, $T_{g,\alpha}$ merges with $T_{g,\beta}$; as a result, only one T_g is observed at higher AdA fractions. In our previous study [31], two thermal anomalies are observed for PDiPF at 79 °C and 137 °C, respectively, during the first heating process at a rate of 10 K/min from differential scanning calorimetry (DSC) measurements. Furthermore, DMA measurements [30] revealed the presence of two mechanical anomalies at $T_\beta = 80$ °C and $T_\alpha = 220$ °C for PDiPF, where the frequency of the applied sinusoidal strain is 2 Hz. With the increase in the AdA fraction, T_α and T_β approach each other. The AdA fraction dependence of $T_{g,\alpha}$ and $T_{g,\beta}$ in Fig. 7 is consistent with that observed by DSC and DMA.

For P(DiPF/nBA), with the increase in the nBA fraction, $T_{g,\alpha}$ and $T_{g,\beta}$ decrease (See purple squares □ and green circles ○). For P(DiPF/nBA) with nBA fraction of 11%, 65%, and 81%, the α-process is not observed because the dielectric strength of the α-process is weak, and the α-process is overlapped with a large contribution from DC conductivity. With higher nBA fractions, only one relaxation process is observed, except for the γ-process.

As for DSC measurements, additional results should be added to discuss the origin of the α- and β-processes. During the second (third) heating process on PDiPF, thermal anomaly around 68 °C is observed, while the thermal anomaly around 137 °C becomes too weak to be observed. The temperature T_{DSC} at which the thermal anomaly could be observed during the second (third) heating and cooling processes are measured as a function of AdA or nBA fractions. The values of T_{DSC} are listed in Table 1 and plotted as gray symbols in Fig. 7.

Next, the Vogel temperatures T_0, at which the relaxation times of the α- or β-process increase anomalously, are plotted as a function of fractions of acrylate segments (Fig. 8). For PDiPF, the Vogel temperature evaluated from the α-process, $T_{0,\alpha}$, is almost the same as that from the β-process, $T_{0,\beta}$. *This coincidence in the Vogel temperature between the α- and β-processes suggested that the physical origin of the α-process is the same as that of the β-process for the PDiPF homopolymer.* With the increase in the AdA fraction, the Vogel temperature $T_{0,\alpha}$ decreases, while $T_{0,\beta}$ increases. For PAdA (AdA = 100%), $T_{0,\alpha}$ is apparently so low that $T_{0,\alpha}$ can be regarded as nearly zero, although there are large statistical errors. This result possibly suggested that the relaxation times of the α-process for PAdA can be described by the Arrhenius law, not by the VFT law. For P(DiPF/nBA), with the increase in the nBA fraction, the Vogel temperature $T_{0,\beta}$ decreases. The final value of $T_{0,\beta}$ is greater than that observed for PAdA.

Here, T_g exhibits AdA or nBA fraction dependence different from that of T_0, although T_g and T_0 are parameters that characterize the glass transition behavior. Because T_0 is strongly associated with fragility, this is the case where the fragility index exhibits different dependence on the AdA or nBA fraction.

In our previous study [31], dynamics of the β-process and the packing structure for PDiPF have been reported to exhibit an anomalous behavior in comparison with those observed for typical acrylate polymers as follows: 1) The relaxation times of the β-process of PDiPF obey the VFT law, 2) a clear step is observed at $T_{g,\beta}$ in the DSC curve, and 3) the microscopic packing of the polymer chains is enhanced in the solid state. Furthermore, the current DRS measurement revealed that the coincidence of the Vogel temperature between the α- and β-processes is observed, which should be correlated with anomalous behavior observed by DRS, DMA, and DSC in a previous study.

Notably, the PAdA homopolymer also exhibits unusual dynamics because the dynamics of the α-process might be approximately described by the Arrhenius law, while the β-process can well be described by the VFT law. P(DiPF/AdA) is a copolymer of the two "unusual" polymers, PDiPF and PAdA.

3.3.2. Angell plot and fragility

Glassy dynamics in amorphous materials are often discussed on the basis of a scaling plot such as the Angell plot [39–41]. In the plot, the temperature dependence of the relaxation times of the α-process (in our study, the β-process as well) can be scaled with respect to the values at $T_{g,i}$ where $\tau_i = \tau_g$ and $i = \alpha, \beta$.

Fig. 9 shows the Angell plot for the α- and β-processes of P(DiPF/AdA) copolymers, where the values of $\log_{10}[\tau_\alpha/\tau_g]$ and $\log_{10}[\tau_\beta/\tau_g]$ are plotted as a function of $T_{g,\alpha}/T$ and $T_{g,\beta}/T$, respectively, under the condition that $\tau_g = 10^2$ s. The scaled relaxation times of the α-process for five AdA fractions are located in a narrow region, while those of the β-process are located in a wider region, and the dependence of $\tau_\beta(T)$ on

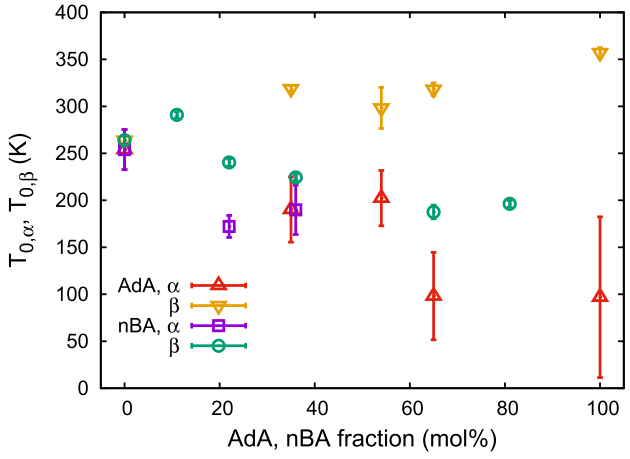

Fig. 8. AdA or nBA fraction dependence of the Vogel temperature T_0 evaluated from the temperature dependence of the relaxation rate of the α- and β-processes for P(DiPF/AdA) and P(DiPF/nBA). Here, the Vogel temperatures $T_{0,\alpha}$ and $T_{0,\beta}$ are defined in Eq. (5).

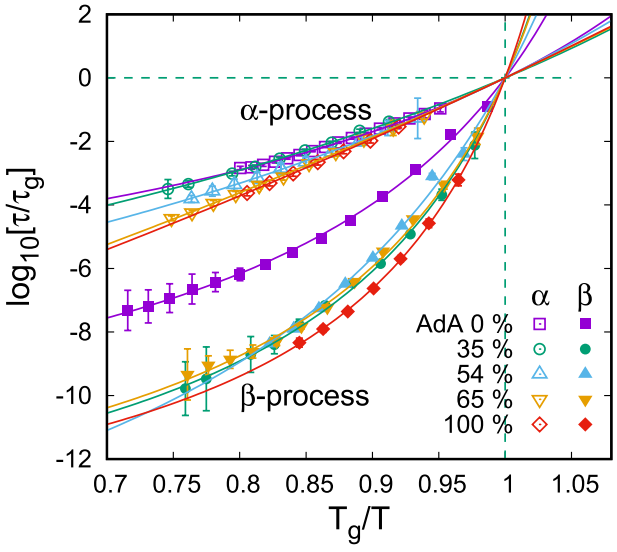

Fig. 9. Angell plots of the relaxation time of the α- and β-processes for DiPF/AdA copolymers with various fractions of AdA. The glass transition temperature T_g is defined as the temperature at which the relaxation time of the α-process or β-process is equal to 10^2 s ($\equiv \tau_g$).

the AdA fraction is considerably stronger than that of the α-process (Fig. 9).

The deviation of the β-process from the Arrhenius law, that is, the straight line in this plot, seems to be considerably greater than that of the α-process (Fig. 9). The degree of deviation is apparently dependent on the AdA fraction for P(DiPF/AdA) copolymers. Fig. S4 in the Supplemental Material shows the Angell plots of the α- and β-processes for P(DiPF/nBA).

The fragility index can be used to quantify the deviation of the dynamics from the Arrhenius law for glassy systems. In our case, the fragility index m can be evaluated from the fitting parameters of Eq. (5) in addition to $T_{g,\alpha}$ or $T_{g,\beta}$, using the following equation [42]:

$$m = \left[\frac{d\log_{10}\tau_i(T)}{d(T_{g,i}/T)}\right]_{T=T_{g,i}}. \quad (6)$$

The fragility index is equal to the slope at T_g of the scaled curve in the Angell plot, and it can be used to classify the glassy dynamics based on the observed temperature dependence of the relaxation times of the dynamical processes.

Fig. 10 shows the AdA or nBA fraction dependence of the fragility index evaluated from the α- and β-processes for P(DiPF/AdA) and P(DiPF/nBA). For PDiPF, the fragility indices of the α- and β-processes are 20 and 53, respectively. With the increase in the AdA fraction from 0 to 100%, the fragility index of the α-process remains almost constant regardless of the AdA fractions, while that of the β-process increases with AdA fraction to reach 112 for PAdA. This result suggested that the glassy dynamics related to the β-process change to *more fragile* with the increase in the AdA fractions. For P(DiPF/nBA), the fragility index of the β-process exhibits a similar dependence on the nBA fraction.

3.3.3. *Merging of the α- and β-processes and the origin of the β-process*

Here, we would like to discuss the dynamics of the α- and β-processes for P(DiPF/AdA) and P(DiPF/nBA) copolymers in more detail. First, for PDiPF, the following results are obtained: 1) The relaxation times of the α- and β-processes obey the VFT law, and 2) The Vogel temperature for the α-process is nearly equal to that of the β-process. This result indicates that there is a strong correlation between the α- and β-processes for PDiPF. Even after the addition of an acrylate segment of AdA, α- and β-processes exist, and the two processes are apparently correlated. Fig. 11 shows the temperature dependence of the normalized relaxation strengths of the α- and β-processes for P(DiPF/AdA) with various AdA fractions. The relaxation strength of the α-process increases with the increase in the temperature, while that of the β-process decreases,

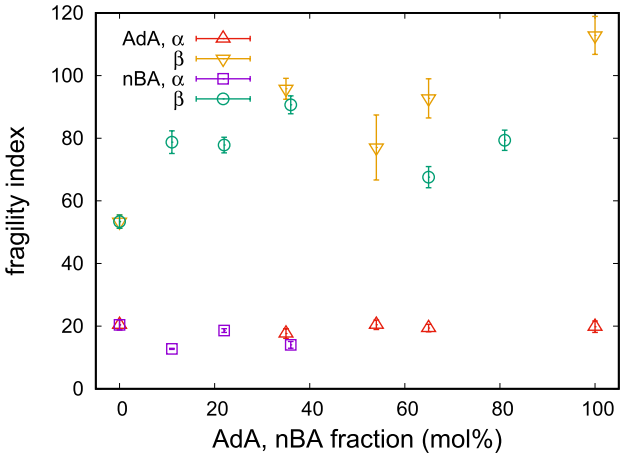

Fig. 10. AdA or nBA fraction dependence of the fragility index evaluated from the relaxation rate of the α- and β-processes for P(DiPF/AdA) and P(DiPF/nBA) copolymers using Eq. (6).

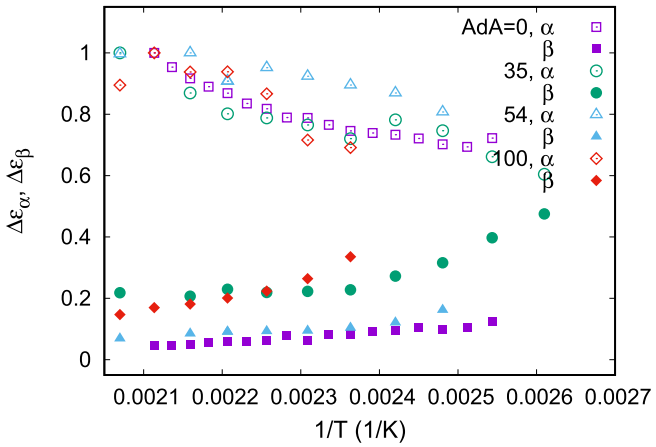

Fig. 11. Dielectric relaxation strength of the α- and β-processes as a function of $1/T$ for P(DiPF/AdA) copolymers. The vertical axis is scaled so that at a higher temperature T_a, the sum of the dielectric relaxation strengths of the α- and β-processes is equal to 1.0. Here, the value of T_a is selected for each AdA fraction.

suggesting that the α- and β-processes can compensate each other.

In Fig. 6, the α-process is separated from the β-process at high temperature, and with the decrease in the temperature to the glass transition temperature, the two processes approach each other. In typical amorphous materials including polymeric systems, two dynamical modes, the α- and β-processes at low temperatures near T_g exist, respectively, while the β-process merges with the α-process at high temperatures [43,44]. Hence, the merging of the α- and β-processes in the current system may have properties different from ordinary ones.

For PnBA, only one relaxation process exists in addition to the γ-process [37]. The process is assigned to the "α-process", where the segmental motion of the main chains is coupled with the rotation of the side group (the "β-process"). In Fig. 5(b), the "α-process" and γ-process for PnBA are plotted as the purple down triangle ▽ and the green down triangle ▽, respectively.

For P(DiPF/nBA), the β-process is observed in addition to the γ-process for all nBA fractions, and the α-process also is observed for nBA fractions less than or equal to 36% (Fig. 5(b) and Fig. S3 in the Supplemental Material). The curve for the "α-process" of PnBA smoothly changes to that for the β-process of P(DiPF/nBA) with the decrease in the nBA fraction and finally reaches that of the β-process of PDiPF.

Furthermore, DSC measurements show that thermal anomaly can be observed at the temperaure T_{DSC}. The dependences of the T_{DSC} on AdA or nBA fraction are shown in Table 1 and Fig. 7. Although there are some differences depending on whether the measurement is performed during the heating or cooling process, the dependence of the temperaure T_{DSC} on AdA or nBA fraction seems to be similar to that of $T_{g,\beta}$.

Therefore, it is reasonable to assume that the β-process for PDiPF should be primary dispersion, which is associated with the segmental motion of the PDiPF homopolymer, judging from the apparent nBA fraction dependence of the dynamical processes measured by DRS and the results obtained by DSC.

3.3.4. *Origin of the α-process*

Next, we will discuss the origin of the α-process for PDiPF. As already mentioned, the VFT law is also valid for α- and β-processes. If the β-process is the primary dispersion related to segmental motion, the α-process should be associated with a motion slower than segmental motion. There are some possible candidates for the α-process of PDiPF. First is the normal-mode motion of polymer chains [45,46]. However, PDiPF is not an A-type polymer; hence it is difficult to observe this motion by DRS in principle. Furthermore, DMA measurements were

performed to investigate the α-process for poly(diethyl fumarate) (PDEF) with various molecular weights [47]. The structure of PDEF is similar to that of PDiPF except for the number of methyl groups at the end of the side group. Hence, similar dynamics can be expected for PDiPF and PDEF. With the increase in the molecular weight, the α-relaxation temperature observed at 2 Hz for PDEF increases and then saturates to a constant value at a molecular weight greater than ~70, 000. This result suggested that there is a low possibility that the normal mode is the origin of the α-process for PDiPF.

Second is the conformational dynamics except the normal mode, where dynamics is not entire motion of polymer chains, but the motion extended over several segments with a time scale longer than that of the segmental motion. This type of motion has been reported first from NMR data [48,49], and DRS measurements also reveal the presence of this motion for poly(2-vinyl pyridine), which is referred to as the *slower process* [50]. The relaxation time of the slower process is greater than that of the segmental motion at high temperatures, while the difference between the two relaxation times becomes less by approaching to T_g from the higher-temperature side. The slower process may be more suitable candidate for the origin of the α-process, although more detailed measurements such as NMR will be considerably required for this purpose.

Here, it should be noted that the α-process is located at high temperature and low frequency regions and is overlapped with the contribution from the DC conductivity. Because the mechanical measurements clearly show the existence of dynamical process of polymer chains at the region where the α-process is observed, the physical origin of the α-process can be expected to be correlated with a molecular motion of polymers. At the same time, a motion of charge carriers which exist within polymeric systems as space charges could not necessarily be neglected. On the contrary, there might be a possibility of the coupling of charge carrier motion with molecular motion of polymers. This possibility has to be taken into account when discussing the physical origin of the α-process. To clarify this issue, we plan to perform further dielectric measurements on the α-process under controlled DC conductivity.

At the end of this section, a remark on the α- and β-processes of PAdA is given as follows. For PAdA, Fig. 6 shows that *there must be an intersection between the α- and β-processes* at $1/T \approx 0.00242K^{-1}$ and $f \approx 0.05$ Hz. If this is correct, at a frequency below the intersection frequency, T_α is less than T_β. Depending on the frequency, the "α-process" can be replaced by the "β-process" and vice versa. Such an intersection of the two relaxation processes is observed for supercooled ethylcyclohexane [51,52]. In that system, the secondary relaxation process is persistent even in the liquid state at slow relaxation times. If this scenario is valid for PAdA, this might be another possible candidate for the origin of the α-process of PDiPF.

3.4. γ-process

In this section, the properties of the γ-process are discussed for the two copolymers. Fig. 12 shows the temperature dependence of the relaxation rates of the γ-process observed for (a) P(DiPF/AdA) and (b) P(DiPF/nBA). The relaxation rate of the γ-process for PDiPF cannot be fitted by a single straight line for all temperature ranges (Fig. 12(a)). At high temperatures, there is a deviation from the straight line drawn in the low-temperature region, which might be related to a correlation between the γ- and β-processes. However, in the discussion below, the deviation at high temperatures is neglected, and the fitting by the Arrhenius law was performed for the data points in the lower-temperature region.

With the increase in the AdA fraction, the relaxation rate of the γ-process at a given temperature increases continuously for P(DiPF/AdA), as shown in Fig. 12(a). On the other hand, with the increase in the AdA fraction, $T_{g,\beta}$ increases (Fig. 7), and hence, with the increase in this fraction, the mobility of the main chain is considered to decrease. Thus,

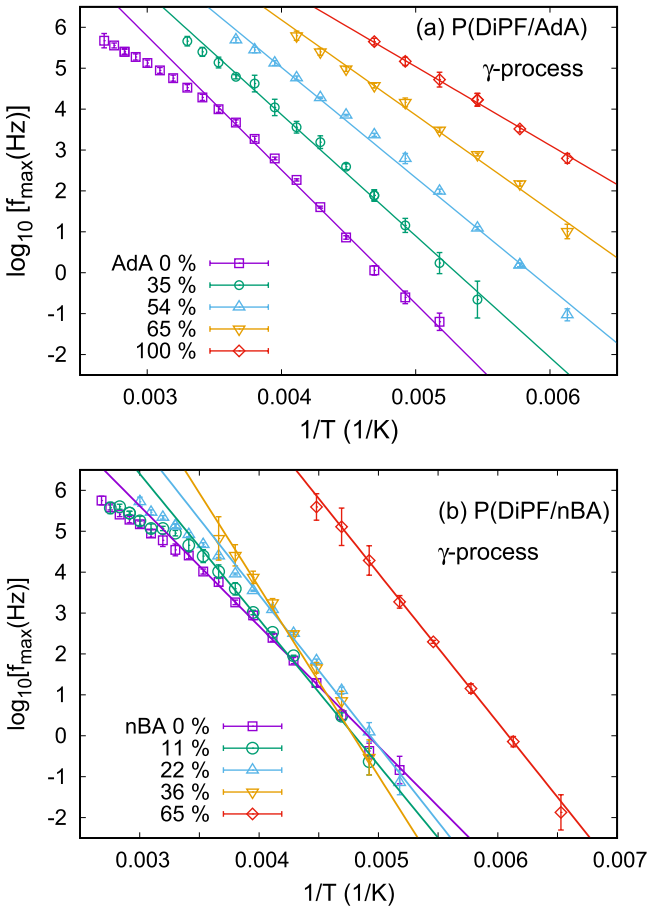

Fig. 12. Relaxation rate of the γ-process as a function of the inverse of temperature for (a) P(DiPF/AdA) and (b) P(DiPF/nBA) with various fractions of acrylate segments. The straight lines are obtained using Eq. (5) with $T_0 = 0$ *K*.

the increase in the relaxation rate of the γ-process may suggest that the γ-process is negatively affected by the main chain motion. If the γ-process exhibits a completely local nature, the copolymers should exhibit two γ-processes, originating from DiPF and AdA segments, and the relaxation strengths of the two processes should be determined by the DiPF and AdA fractions. Nevertheless, the result in Fig. 12(a) is contrary to the above expectation. In this case, the motional unit is not a single side group, but two or more neighboring side groups correlated via some segments of the backbone chain.

X-ray scattering revealed that the WAXS pattern continuously changes with the AdA fraction (Fig. 2(a)), suggesting that the packing order in P(DiPF/AdA) continuously changes with the AdA fraction, possibly leading to the continuous change in the dynamics of the γ-process. Fig. 13 shows the relaxation rate of the γ-process and the peak position of the second peak in the WAXS pattern q_{max} as a function of the AdA fraction. The dynamics of the γ-process are clearly correlated with the structural change. Even for the local dynamics such as the γ-process, there is a correlation between the backbone chain structure and side-group motion.

Fig. 12(b) shows the temperature dependence of the relaxation rate of the γ-process for P(DiPF/nBA). Contrary to P(DiPF/AdA), the γ-process remains at similar positions in the dispersion map with the increase in the nBA fraction up to 36%. However, with the further increase in the nBA fraction to 65%, the γ-process is shifted to the high-frequency and low-temperature side. The γ-process for an nBA fraction of 81% is not observed within the present measurement windows, but only the tail of the dielectric loss peak of the γ-process is observed. For P(DiPF/nBA), the WAXS pattern in Fig. 2(b) revealed that the locations of the two

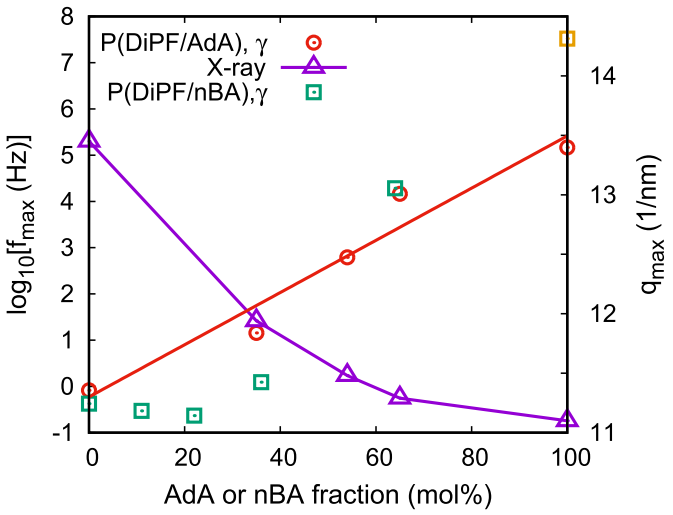

Fig. 13. Relaxation rate of the γ-process at 203 K as a function of the AdA or nBA fraction for P(DiPF/AdA) (○) and P(DiPF/nBA) (□), and the peak position of the second peak in the WAXS pattern q_{max} for P(DiPF/AdA)(△). The symbol □ denotes the relaxation rate of the γ-process at 203 K for PnBA, which can be found from Ref. [37].

scattering peaks do not change, and only the intensity ratio of the two peaks changes with the increase in the nBA fraction. From these results, we could speculate on the properties of the γ-process as follows. For P(DiPF/nBA), there could be two γ-processes: one originates mainly from the DiPF segment, and the other does mainly from the nBA segment. The γ-process from the DiPF segment has a distinct character independent of the nBA segment. On the other hand, the γ-process from the nBA segment has less independence of DiPF segment or other circumstances, and hence the location in the dispersion map changes sensitively to the change in nBA fraction. Because two γ-processes cannot be observed for low nBA fractions in the present measurements, the γ-process originated from nBA segment is totally merged with the one from DiPF segment for lower nBA fraction, while it separates from the γ-process originated from DiPF segment for high nBA fractions where the strength of γ-process from DiPF segment is so small that it could not be observed. Probably there might be a possibility that two γ-processes could be observed if the nBA fraction is chosen appropriately so that the strength of the γ-process from DiPF segment can still be large enough and the location of the γ-process from nBA segment is well separated enough from that of the γ-process from DiPF segment.

Clearly, the difference between P(DiPF/AdA) and P(DiPF/nBA) should originate from the difference in the dynamical character between the two acrylate segments. The specific rigidity and high symmetry of the adamantyl group [53,54] may induce the cooperativity of the side-chain motion among the adamantyl group, the diisopropyl group, and backbone chains.

The activation energies of the γ-process evaluated from the data fitting using the Arrhenius law are 0.9 ~1.5 kJ/mol (Table 1). The values are consistent with those reported for side-chain motion [55]. A possible origin of the γ-process can be the rotation of a part of the side group around the C–O bond, where the C is the carbon atom in the side group nearest to the backbone chain, if we consider the dielectric activeness of the motion. From the above discussion, the part of the side group does not rotate independently, but with some correlation with some segments of the backbone chain.

4. Concluding remarks

In this study, DRS measurements of two copolymers of DiPF with AdA and nBA in addition to X-ray scattering experiments are performed to elucidate the effect of the induction of a structural constraint by the absence of a CH_2 spacer in the backbone chain on the dynamics of a polymer chain. PDiPF exhibits three dynamical processes: α-, β-, and γ-processes. The relaxation times of α- and β-processes can be described by the VFT law. From the above discussions, it is reasonable to assign segmental motions of the main chains to the origin of the β-process observed for PDiPF. Thus, segmental motion should be considered to be unfrozen in the temperature range above $T_{g,\beta}$. However, the elastic modulus of PDiPF *even in the temperature region between* T_α *and* T_β at a frequency is so high that in this temperature region, PDiPF can be regarded as solid, not a liquid, and then above T_α, PDiPF finally changes to the liquid state with a lower elastic modulus [30]. This behavior is quite unusual, which must be related to the structural constraint.

Some candidates can be responsible for the origin of the α-process, as discussed in Sec. 3.3. Here, an additional comment on this point is as follows. Locations of the α-process in the dispersion map are in the limited region, and the fragility index of the α-process is ~20 regardless of the AdA fractions. Hence, apparently, there is a common physical origin for the α-process for PDiPF and PAdA. For P(DiPF/AdA), the α- and β-processes in the dispersion map seem to change continuously with the AdA fraction in Fig. 6. With the increase in the AdA fraction, $T_{g,\beta}$ increases, and the curve of the relaxation rate of the β-process tends to intersect with that of the α-process in the low-frequency and low-temperature region.

As mentioned in Sec. 1, we adopt conventional notation of the relaxation processes. However, the present experimental result suggests that the β-process is associated with the segmental motion. Hence, it might be better to call the β-process as 'the α-process', and the α-process as 'the slower process', respectively, in order to judge the physical origin of the process only from the name. At the same time, we noticed that the elastic modulus between T_α and T_β is so high that PDiPF can be regarded as solid for this temperature range, although the segmental motion is already activated. This suggests that the dynamics of the segmental motion in PDiPF is something different from the typical segmental motion in many amorphous polymers.

Declaration of competing interest

The authors declare that they have no known competing financial interests or personal relationships that could have appeared to influence the work reported in this paper.

Acknowledgements

This work was supported by a Grant-in-Aid for Scientific Research (B) (Grant No. 19H01865) and Exploratory Research (Grant No. 18K18740) from the Japan Society for the Promotion of Science. Synchrotron radiation experiments were performed at the BL40B2 of SPring-8 with the approval of the Japan Synchrotron Radiation Research Institute (JASRI) (Proposals No. 2017B1119, No. 2018B1454, No. 2019A1301, and No. 2019B1226).

Appendix A. Supplementary data

Supplementary data to this article can be found online at https://doi.org/10.1016/j.polymer.2022.124671.

References

[1] N. McCrum, B. Read, G. Williams, Anelastic and Dielectric Effects in Polymeric Solids, Dover Books on Engineering, Dover Publications, 1967.
[2] G.R. Strobl, Mechanical and dielectric response, in: The Physics of Polymers, Springer-Verlag Berlin Heidelberg, 2007, pp. 223–286.
[3] M.D. Ediger, C.A. Angell, S.R. Nagel, Supercooled liquids and glasses, J. Phys. Chem. 100 (1996) 13200–13212.
[4] K.L. Ngai, The glass transition and the glassy state, in: J. Mark (Ed.), Physical Properties of Polymers, Cambridge University Press, 2004, pp. 72–152.
[5] H. Vogel, Das temperatur-abhängigkeitsgesetz der viskosität von flüssigkeiten, Phys. Z. 22 (1921) 645–646.

[6] G.S. Fulcher, Analysis of recent measurements of the viscosity of glasses, J. Am. Ceram. Soc. 8 (1925) 339–355.
[7] G.S. Fulcher, Analysis of recent measurements of the viscosity of glasses.–ii1, J. Am. Ceram. Soc. 8 (1925) 789–794.
[8] G. Tammann, W. Hesse, Die abhängigkeit der viscosität von der temperatur bie unterkühlten flüssigkeiten, Z. Anorg. Allg. Chem. 156 (1926) 245–257.
[9] K. Yamafuji, Y. Ishida, Dielectric α_a- and β_a-absorptions in some amorphous and semi-crystalline polymers, Kolloid Z. Z. Polym. 183 (1962) 15–37.
[10] S. Saito, Temperature dependence of dielectric relaxation behavior for various polymer systems, Kolloid Z. Z. Polym. 189 (1963) 116–125.
[11] G.P. Johari, M. Goldstein, Molecular mobility in simple glasses, J. Phys. Chem. 74 (1970) 2034–2035.
[12] M. Goldstein, Viscous liquids and the glass transition: a potential energy barrier picture, J. Chem. Phys. 51 (1969) 3728–3739.
[13] G.P. Johari, M. Goldstein, Viscous liquids and the glass transition. ii. secondary relaxations in glasses of rigid molecules, J. Chem. Phys. 53 (1970) 2372–2388.
[14] G.P. Johari, M. Goldstein, Viscous liquids and the glass transition. iii. secondary relaxations in aliphatic alcohols and other nonrigid molecules, J. Chem. Phys. 55 (1971) 4245–4252.
[15] A.S. Kulik, H.W. Beckham, K. Schmidt-Rohr, D. Radloff, U. Pawelzik, C. Boeffel, H. W. Spiess, Coupling of α and β processes in poly(ethyl methacrylate) investigated by multidimensional nmr, Macromolecules 27 (1994) 4746–4754.
[16] K. Schmidt-Rohr, A.S. Kulik, H.W. Beckham, A. Ohlemacher, U. Pawelzik, C. Boeffel, H.W. Spiess, Molecular nature of the β relaxation in poly(methyl methacrylate) investigated by multidimensional nmr, Macromolecules 27 (1994) 4733–4745.
[17] M. Rubinstein, R.H. Colby, Polymer Physics, Oxford University Press, 2003.
[18] C.B. Roth, Polymer Glasses, CRC Press, 2016.
[19] Y. Ishida, K. Yamafuji, Studies on dielectric behaviors in a series of polyalkyl-methacrylates, Kolloid Z. 177 (1961) 97–116.
[20] J. Heijboer, Mechanical properties and molecular structure of organic polymers, in: J.A. Prins (Ed.), Physics of Non-crystalline Solids, North-Holland, Amsterdam, 1965, pp. 231–253.
[21] R. Bergman, F. Alvarez, A. Alegria, J. Colmenero, The merging of the dielectric α- and β-relaxations in poly-(methyl methacrylate), J. Chem. Phys. 109 (1998) 7546–7555.
[22] R. Bergman, F. Alvarez, A. Alegria, J. Colmenero, Dielectric relaxation in pmma revisited, J. Non-Cryst. Solids 235–237 (1998) 580–583.
[23] K. Fukao, S. Uno, Y. Miyamoto, A. Hoshino, H. Miyaji, Dynamics of α and β processes in thin polymer films: poly(vinyl acetate) and poly(methyl methacrylate), Phys. Rev. E 64 (2001), 051807.
[24] T. Otsu, O. Ito, N. Toyoda, S. Mori, Polymers from 1,2-disubstituted ethylenic monomers, 2. homopolymers from dialkyl fumarates by radical initiator, Makromol. Chem., Rapid Commun. 2 (1981) 725–728.
[25] N. Toyoda, T. Otsu, Polymers from 1,2-disubstituted ethylenic monomers. ix. radical high polymerization of methyl-tert-butyl fumarate, J. Macromol. Sci., Chem. 19 (1983) 1011–1021.
[26] T. Otsu, K. Shiraishi, A. Matsumoto, Radical polymerization and copolymerization reactivities of fumarates bearing different alkyl ester groups, J. Polym. Sci. Polym. Chem. 31 (1993) 2523–2529.
[27] T. Otsu, T. Yasuhara, K. Shiraishi, S. Mori, Radical high polymerization of di-tert-butyl fumarate and novel synthesis of high molecular weight poly(fumaric acid) from its polymer, Polym. Bull. 12 (1984) 449–456.
[28] A. Matsumoto, T. Tarui, T. Otsu, Dilute solution properties of semiflexible poly (substituted methylenes): intrinsic viscosity of poly(diisopropyl fumarate) in benzene, Macromolecules 23 (1990) 5102–5105.
[29] A. Matsumoto, E. Nakagawa, Evaluation of chain rigidity of poly(diisopropyl fumarate) from light scattering and viscosity in tetrahydrofuran, Eur. Polym. J. 35 (1999) 2107–2113.
[30] Y. Suzuki, T. Tsujimura, K. Funamoto, A. Matsumoto, Relaxation behavior of random copolymers containing rigid fumarate and flexible acrylate segments by dynamic mechanical analysis, Polym. J. 51 (2019) 1163–1172.
[31] Y. Suzuki, K. Miyata, M. Sato, N. Tsuji, K. Fukao, A. Matsumoto, Relaxation behavior of poly(diisopropyl fumarate) including no methylene spacer in the main chain, Polymer 196 (2020) 122479.
[32] K. Yamada, M. Takayanagi, Y. Murata, Relations between molecular aggregation state and mechanical properties in poly(diisopropyl fumarate), Polymer 27 (1986) 1054–1057.
[33] N. Taniguchi, K. Fukao, P. Sotta, D.R. Long, Dielectric relaxation of thin films of polyamide random copolymers, Phys. Rev. E 91 (2015), 052605.
[34] K. Matsuura, K. Kuboyama, T. Ougizawa, Interfacial region of poly(n-butyl acrylate)/silicon oxide, J. Appl. Polym. Sci. 138 (2021) 50268.
[35] S. Havriliak, S. Negami, A complex plane representation of dielectric and mechanical relaxation processes in some polymers, Polymer 8 (1967) 161–210.
[36] F. Kremer, A. Schönhals, Analysis of dielectric spectra, in: Broadband Dielectric Spectroscopy, Springer-Verlag Berlin Heidelberg, 2003, pp. 59–98.
[37] T. Hayakawa, K. Adachi, Dielectric relaxation of poly(n-butyl acrylate), Polym. J. 32 (2000) 845–848.
[38] K. Fukao, H. Takaki, T. Hayashi, Heterogeneous dynamics of multilayered thin polymer films, in: F. Kremer (Ed.), Dynamics in Geometrical Confinement, Advances in Dielectrics, Springer International Publishing, 2014, pp. 179–212.
[39] C. Angell, Strong and fragile liquids, in: K.L. Ngai, G. Wright (Eds.), Relaxations in Complex Systems, National Technical Information Service, U.S., 1985, pp. 3–16.
[40] C. Angell, Relaxation in liquids, polymers and plastic crystals – strong/fragile patterns and problems, J. Non-Cryst. Solids 131–133 (1991) 13–31 (Proceedings of the International Discussion Meeting on Relaxations in Complex Systems).
[41] I.M. Kalogeras, H.E.H. Lobland, The nature of the glassy state: structure and glass transitions, J. Mater. Educ. 34 (2012) 69–94.
[42] R. Böhmer, C.A. Angell, Correlations of the nonexponentiality and state dependence of mechanical relaxations with bond connectivity in ge-as-se supercooled liquids, Phys. Rev. B 45 (1992) 10091–10094.
[43] G. Williams, Dipole relaxation in polyethyl methacrylate and polyethyl acrylate as a function of frequency, temperature and pressure. the α, β and $\alpha\beta$ relaxations, Trans. Faraday Soc. 62 (1966) 2091–2102.
[44] M. Beiner, Relaxation in poly(alkyl methacrylate)s: crossover region and nanophase separation, Macromol. Rapid Commun. 22 (2001) 869–895.
[45] W.H. Stockmayer, M.E. Baur, Low-frequency electrical response of flexible chain molecules, J. Am. Chem. Soc. 86 (1964) 3485–3489.
[46] D. Boese, F. Kremer, Molecular dynamics in bulk cis-polyisoprene as studied by dielectric spectroscopy, Macromolecules 23 (1990) 829–835.
[47] Y. Suzuki, N. Tsuji, K. Miyata, T. Kano, K. Fukao, A. Matsumoto, Characteristic features of α and β relaxations of poly(diethyl fumarate) as the poly(substituted methylene), Macromol. Chem. Phys. 222 (2021) 2100124.
[48] M. Wind, R. Graf, A. Heuer, H.W. Spiess, Structural relaxation of polymers at the glass transition: conformational memory in poly(n-alkylmethacrylates), Phys. Rev. Lett. 91 (2003) 155702.
[49] C. Friedrichs, S. Emmerling, G. Kircher, R. Graf, H. Wolfgang Spiess, Glass transition of poly(ethylmethacrylate) admixed and bound to nanoparticles, J. Chem. Phys. 138 (2013) 12A503.
[50] P. Papadopoulos, D. Peristeraki, G. Floudas, G. Koutalas, N. Hadjichristidis, Origin of glass transition of poly(2-vinylpyridine). a temperature- and pressure-dependent dielectric spectroscopy study, Macromolecules 37 (2004) 8116–8122.
[51] A. Mandanici, M. Cutroni, Multiple mechanical relaxations in ethylcyclohexane above the glass transition temperature, J. Phys. Chem. B 111 (2007) 10999–11003.
[52] A. Mandanici, W. Huang, M. Cutroni, R. Richert, Dynamics of glass-forming liquids. xii. dielectric study of primary and secondary relaxations in ethylcyclohexane, J. Chem. Phys. 128 (2008) 124505.
[53] A. Matsumoto, S. Tanaka, T. Otsu, Synthesis and characterization of poly(1-adamantyl methacrylate): effects of the adamantyl group on radical polymerization kinetics and thermal properties of the polymer, Macromolecules 24 (1991) 4017–4024.
[54] Y. Nakano, E. Sato, A. Matsumoto, Synthesis and thermal, optical, and mechanical properties of sequence-controlled poly(1-adamantyl acrylate)-block-poly(n-butyl acrylate) containing polar side group, J. Polym. Sci.: Polym. Chem. 52 (2014) 2899–2910.
[55] Y. Kawamura, S. Nagai, J. Hirose, Y. Wada, Study of the side-chain relaxation of methacrylate homopolymers and copolymers by the dielectric method, J. Polym. Sci. 2 Polym. Phys. 7 (1969) 1559–1575.